Pak. j. sci. ind. res. Ser. A: phy. sci. 2023 **66A**(2) 180-200

# Heat Transfer Optimization in Car Radiator Using Nanofluid

**Syed Muhammad Tariq[a], Asim Mushtaq[b]*, Ahmed Ullah[a], Rizwan Ahmed Qamar[b] and Zaeem Uddin Ali[d]**
[a]Chemical Engineering Department, NED University of Engineering and Technology, Karachi, Pakistan
[b]Polymer and Petrochemical Engineering Department, NED University of Engineering and Technology, Karachi, Pakistan

(received May 5, 2021; revised June 6, 2022; accepted June 13, 2022)

**Abstract.** This research focused on applying water and ethylene glycol based alumina nanofluid for heat transfer enhancement in the car radiator. Firstly, simulated the water to validate the model. Then moved on to the nanofluids simulation and worked on different nanoparticle concentrations 1, 1.5, 2.5, 3.5 and 4%. All concentrations showed heat transfer enhancement compared with the pure base fluid. The Reynolds number of the water and the water based nanofluids ranges from (10000-30000 $R_e$) and the Reynolds number for the ethylene glycol and the ethylene glycol based nanofluids ranges from (1000-3000 $R_e$). A higher Reynolds number resulted in more significant heat transfer. The Nusselt number has a direct relation with the concentration. As the concentration of the nanofluid increases, the Nusselt number also increases.

**Keywords:** radiator, ethylene glycol, Reynolds number, Nusselt number, nanofluid

## Introduction

Preceding the Second World War plain water was utilized as a coolant for the car business. Water was a great choice as it was generally accessible just as being cost effective. Nonetheless, with the improvement of the powerful airplane for military and local purposes the water would boil, prompting harm and engine failure. What was required was a substance that raised the breaking point of water to a lot more elevated. Ironically, antifreeze which had been utilized in winter to prevent the engine from freezing over which was viable at doing this and is still generally used today. After some time, different added substances were likewise blended with the water and liquid catalyst, for example, erosion inhibitors that help expand the life of a metal or alloy by reducing the rate at which they consume. It is precious as it keeps the coolant from doing any harm to the engine (Mandole *et al*., 2020, Patil *et al*., 2017).

The nanofluids invented in 1995 at Argonne National Laboratory. The addition of copper nanoparticles to the base fluid, there was a dramatic increase in the thermal conductivity of the resultant fluid and the addition of 5%, CuO to water 60% increase in thermal conductivity was obtained. After addition of CuO field of nanofluids, types of nanofluids are given in Table 1 (Al-Araji *et al*., 2021, Patil *et al*., 2017). These fluids will play an essential role in the development of following generation cooling technologies. The results can be highly conducted and stable and will give the newer application in the future. It was evident from the coolants' thermal properties used today for the heat transfer that they have low heat conductivity. In an automobile, an engine is a essential part because it is responsible for the car to work by converting chemical energy into mechanical energy. This research analyzes heat transfer optimization in car radiators using different nanofluids, using various base fluids and using different nanofluids concentrations (Mert *et al*., 2021; Ahmed *et al.* 2020).

The coolant being used in the radiator is mainly water but these days to enhance heat transfer, nanofluids are being used. Nanofluids are used now adays in various fields like cooling in industries, sensors, cooling of microchips and cooling car engines and radiators. Most companies like "NANOHEX" and "TriboTex" use nano-fluids for car radiators and engines. By using nanofluids in the car, the radiator can reduce its size of radiator. Argonne researchers determined that using high thermal conductive fluids in radiators can reduce the frontal area by 10%. It can lead to fuel saving by 5% and corrosion rate also decreases by using these nanofluids. Many nanofluids are being used by different companies, like Ford Company has made nanoparticle based fluid for heat transfer enhancement for their car (Ford), nanofluid-X, Delphi and many other companies.

*Author for correspondence;
E-mail: engrasimmushtaq@yahoo.com

**Table 1.** Types of nanofluids

| Nanofluid | Process | Leads |
|---|---|---|
| Cu nanoparticle+transformer oil suspension | Transformer oil mixed with Cu nanoparticles oleic acid (dispersant) | It has an improved heat transfer coefficient |
| Water+Cu nanoparticles suspension | Using water suspension is created, Cu nanoparticles 5%, and Laurate salt to stabilize. | |
| CuO and $Al_2O_3$ in water | CuO nanoparticles and $Al_2O_3$ were formed by gas condensation | Enhanced 10% heat transfer coefficient, $Al_2O_3$ and 12% CuO rise in thermal conductivity |
| Ethylene glycol and $Al_2O_3$ in water | $Al_2O_3$ nanoparticles were dispersed in ethylene glycol | It has an improved heat transfer coefficient, 18% increase in thermal conductivity for $Al_2O_3$ |
| Graphene nano lubricant | Graphene was dispersed in engine oil with few additives | It improved tribological performance |

Advancements are being made in nanofluid usage and they are conquering almost every field in this world day by day (Awais *et al*., 2020, Karimi and Afrand, 2018).

## Material and Methods

Nanofluids contain nano sized particles having novel properties, suspended in a base fluid. These particles can cause metallic, metallic oxides, metallic carbides, or even carbon nanotubes. Common examples used today can be CuO, $TiO_2$, MgO, $Al_2O_3$, graphene, MWCNT, ZnO and many more. The base of fluids is water oil or ethylene glycol. Both aluminum and copper are used in the fins construction for automobile radiators.

As per the types of fluids and sorts of nanoparticles, one can get various nanofluids like cycle extraction nanofluids, ecological (contamination controlling nanofluids), bio and drug nanofluids. Another class of polymer nanofluids, drag diminishing nanofluids, focuses on improved heat transfer, just as flow friction decrease. A broad scope of dynamic self gathering components for nanoscale structures begins from a suspension of nanoparticles in the liquid. The expansion of nanoparticles in fluid strikingly improves the energy transport cycle of the base fluid. Present day nanotechnology permits one to measure and deliver materials with a standard crystallite size <50 nm (Abhilash *et al*., 2021, Abu-Hamdeh *et al*., 2020).

Heat transfer liquids comprising water, mineral oils and ethylene glycol play a crucial demonstration in numerous modern methodologies along with power age, substance cycles, warming and cooling systems, transportation, microelectronics and unique miniature estimated applications. The low heat transfer properties of those liquids are an obstacle in improving the warmth move enlargement and depreciation of the warmth exchangers. Various researchers are detailing unique strategies for heat move improvement. A reformist method of enhancing the heat transfer execution of normal liquids is to suspend different sorts of tiny solid particles, including polymeric particles metallic and non metallic in conventional fluids to shape colloidal (Alqahtani *et al*., 2020, Goudarzi and Jamali, 2017).

The utilization of nanofluids in a plate heat exchanger was concentrated mathematically and tentatively by Pantzali utilizing a laminar stream system. The thermal presentation of the nanofluid comprising 4% CuO nanoparticles was contrasted with pure water. The outcomes demonstrated that, at a given heat transfer rate of nanofluids' volumetric stream rate was lower than for pure water and had a lower drop by pressure. The mathematical two dimentioned investigation of single stage constrained convective warmth move for $Al_2O_3$ and $TiO_2$ nanofluids during a flat counter current two fold line heat exchanger. They detailed that heat transfer expanded with the presence of nanoparticles within the base liquid.

In the two stage methodology, the base liquid and nanoparticles are deliberated in two separate stages at various rates and temperatures. The simulated nanofluids to enforce convection heat transfer at a steady temperature in a miniature channel utilizing a laminar stream. This methodology re-enacts the nanofluids in the micro channel. The conditions of protecting mass, force and energy were addressed for the two stages utilizing the limited volume strategy. The two stage recreation results displayed more heat transfer than the single stage homogeneous model. Thus, the Nusselt quantities of the two stage model were half 80% more prominent than for the single stage method (Mandole *et al*., 2020; Kumar and Krishna, 2017).

The tentatively examined constrained convective heat transfer in a water based nanofluid. Five unique centralizations of nanofluids in the scope of 0.1-1 vol. % have been utilized with a stream rate in the range of 90-120 L/min. The outcome shows an increase in heat transfer of 40-45% contrasted with pure water at the convergence of 1% vol. A three dimensional laminar stream and warmth move with two distinctive nanofluids, $Al_2O_3$ and CuO nanoparticle, in ethylene glycol and water blend circling through the level containers of a car radiator. The mathematical outcomes showed a Reynolds number of 2000 (Abhilash *et al*., 2021; Kumar and Krishna 2017). The rate expansion in the standard heat transfer coefficient over the base liquid for a 10% $Al_2O_3$ nanofluid was 94% and that for a 6% CuO nanofluid was 89%. In another study the forced convective heat transfer experimentation was performed on an automobile radiator using coolant fluid as water, water + ethylene glycol, water + ethylene glycol + $TiO_2$ nanoparticles 0.03% and water + ethylene glycol + $TiO_2$ nanoparticles 0.06%. Optimization of heat transfer parameters was achieved and optimized parameters are obtained. The cooling system in cars is made due to heating up of the engine. Continuous heating can lead to fire hazards as high temperatures can burn the entire car. The following components are required in a car cooling system. However, not all of them are always used, radiators pressure caps, water pumps, cooling fans, reserve tanks, freeze plugs, thermostats and bypass systems (Erdoðan *et al*., 2020, Goudarzi *et al*., 2020; Mandole *et al*., 2020).

**Head and intake manifold gaskets.** All privileged consuming motors have motor square two or three chamber heads. The coupling surfaces where the square and head meet are machined level for a close by exact adequate. However, no proportion of mindful machining will empower them to be water tight or have the choice to hold down start gases from moving away from past the mating surfaces. To close the square to the heads, use a head gasket. The head gasket has a couple of things it needs to pack. The essential concern is the ignition tension in each chamber. Oil and coolant ought to successfully stream among square and head and it is the head gasket's action to safeguard these fluids from pouring out or into the ignition chamber or each other. A head gasket through fragile sheet metal that is ventured with edges incorporating all hole focuses. When the head is set in the balance the head gasket is crammed between them. Various fasteners, called head screws are sunk and fixed down causing the head gasket to beat and structure a tight seal between the head and block. Head gaskets normally misfire if the engine overheats for an upheld period making the chamber contort and releasing tension on the head gasket. It is generally fundamental on motors with cast aluminum heads, which are all forefront motors. A head gasket was displacing begins with the tracking down that the head gasket has failed. There is no way to get an expert to know whether there is another mischief to the chamber head or various sections without first destroying the motor. All the person being referred to knows is that fluid or conceivably start is not being confined (Ijaz *et al*., 2020; Vijayan *et al*., 2019).

The hot coolant is in like manner used to offer heat in the vehicle when required. It is a fundamental and clear structure that joins a more desirable focus which appears similar to a short type of radiator, related to the cooling system of several flexible hoses. A fan called blower inducements air through the warmer center and assistants it through the radiator channels to within the vehicle. The warmth is overseen by a blended entrance that mixes cool external air or at a times cooled air with the hot air overcoming the radiator community. The warming temperature is managed by a mixed entry way that blends cool external air or cooled air with the warmed air getting through the warmer center. A few motors do not utilize an elastic hose. All things being equal, they may use a metal cylinder or have an implicit entry in the facade lodging. Subsequently, they are liable to mileage and ultimately may require supplanting as a feature of routine upkeep, on the off chance that the elastic is starting to look dry and broke or turned out to be delicate and elastic (Vijayan *et al*., 2019; Patil *et al*., 2017).

**Computational fluid dynamics (CFD).** It is the model of liquids designing frameworks utilizing displaying (scientific physical issue definition) and numerical techniques (discretization techniques, solvers, numerical parameters, network ages and so on), that initially, have a liquid issue. To take up keep of this issue, the physical properties by utilizing fluid mechanics. At that point, use numerical circumstances to portray these material properties. The Navier-Stokes equation is the administering situation of CFD. As the Navier-Stokes equation is diagnostic, humans can get it and comprehend them on a bit of paper. Be that as it may, if it needs to fathom this condition by PC and need it to interpret the discretized structure. The interpreters are statistical discretization techniques. There are three strategies to investigate fluid hypothesis examination, trial and re-enactment (CFD). CFD numerous favourable circumstances contrasted with tests are shown in Table 2 (Reddy *et al*., 2019; Subhedar *et al*., 2018).

As CFD has such vast numbers of favorable circumstances, it is as of now for the most part utilized in industry, for example, aviation, car, biomedicine, substance preparation, heat ventilation cool, water power, control age, sports marine and so forth.

**Equation of continuity.** The equation of continuity describes the transfer of any quantity. In fluid mechanics, it's the transport of momentum.

$$\frac{\partial \rho}{\partial t} = -\left(\frac{\partial \rho v_x}{\partial x} + \frac{\partial \rho v_y}{\partial y} + \frac{\partial \rho v_z}{\partial z}\right) \text{.................. (1)}$$

This continuity equation describes the change in fluid density concerning the time at a fixed point in space

**Table 2.** CFD aspects

| Parameter | Simulation (CFD) | Experiment |
|---|---|---|
| Budget | Inexpensive | Exclusive |
| Time | Squat | Elongated |
| Scale | Slightly | Small/middle |
| Data | Altogether | Dignified point |
| Repeatable | Affirmative | Approximately |
| Protection | Indeed | Some perilous |

(Al-Araji *et al*., 2021; Vijayan *et al*., 2019; Patil *et al*., 2017).

**Navier-stokes equation.** The momentum in a control volume is kept constant which implies the conservation of momentum that call the Navier-Stokes equation (Kocheril and Elias, 2020). They stand made on the principle that the sum of forces is equal to the mass times acceleration (Al-Araji *et al*., 2021; Mandole *et al*., 2020; Reddy *et al*., 2019; Patel *et al*., 2017).

$$\Sigma F_x = ma_x,\ \Sigma Fy = ma_y,\ \Sigma F_z = ma_z \text{ .................... (2)}$$

Hence, the Navier-Stokes equations for x, y and z components are:

$$\rho g_x - \frac{\partial \rho}{\partial x} + \mu \frac{\partial^2 u}{\partial x^2} + \mu \frac{\partial^2 u}{\partial y^2} + \mu \frac{\partial^2 u}{\partial z^2} = \rho\left(\frac{\partial u}{\partial t} + u\frac{\partial u}{\partial x} + v\frac{\partial u}{\partial y} + w\frac{\partial u}{\partial z}\right) \text{............. (3)}$$

$$\rho g_y - \frac{\partial \rho}{\partial y} + \mu \frac{\partial^2 v}{\partial x^2} + \mu \frac{\partial^2 v}{\partial y^2} + \mu \frac{\partial^2 v}{\partial z^2} = \rho\left(\frac{\partial v}{\partial t} + u\frac{\partial v}{\partial x} + v\frac{\partial v}{\partial y} + w\frac{\partial v}{\partial z}\right) \text{............. (4)}$$

$$\rho g_z - \frac{\partial \rho}{\partial z} + \mu \frac{\partial^2 w}{\partial x^2} + \mu \frac{\partial^2 w}{\partial y^2} + \mu \frac{\partial^2 w}{\partial z^2} = \rho\left(\frac{\partial w}{\partial t} + u\frac{\partial w}{\partial x} + v\frac{\partial w}{\partial y} + w\frac{\partial w}{\partial z}\right) \text{............. (5)}$$

**Difficulties to solve Navier-stokes equation.** The equation for x, y and z components of velocity but no pressure equation. There is a restriction that the Navier-Stokes equation's solution the velocities calculated from the Navier-Stokes equation must satisfy the continuity equation. The convection term in the momentum equation is nonlinear. It cannot use an equation of state to compute pressure.

**Simple algorithm.** The proposed algorithm in 1972, the simple standards for semi-implicit method for pressure linked equations. Develop an equation for pressure from Navier-Stokes and continuity equation which develop a corrector for the velocity field that satisfies the continuity equation.

**Simple solution loop.** Start with the momentum equation by guessing pressure. Calculate the velocity field from momentum equations. Correct the pressure and use the pressure to precise the velocity that satisfies the continuity equation. Compute energy and turbulence scalar transport equations. These turbulence scalar transport equations update the kinematic viscosity, which then passes into the next loop's momentum equation. If velocities do not satisfy the continuity equation, repeat the cycle.

**Fourier's law of heat conduction.** Consider two large parallel plates with a distance Y apart with a A solid slab of area located between them. Initially, the temperature is $T_O$ throughout. At t = O, the lower plate is slightly heated to a $T_1$ temperature and sustained at that temperature. As time passes, the slab's temperature sketch changes eventually achieving a linear steady state profile. At this point, uniform heat rate Q flows through the slab to keep the $\Delta T = T_1 - T_0$ constant.

$$\frac{Q}{A} = k\,\frac{\Delta t}{Y} \quad (6)$$

The heat flux rate (heat flow per area) through the slab is directly related to the temperature decrease and is inversely relational to the distance among the plates as shown in Fig. 1. Here, k (proportionality constant) is the thermal conductivity of the slab. Heat flux in the positive y direction is denoted by $q_y$ and as the thickness of the slab approaches zero, the equation (6) becomes (Jaliliantabar *et al*., 2021; Li *et al*., 2021; Nagib *et al*., 2019),

$$qy = -k\,\frac{dT}{dy} \quad (7)$$

It is Fourier's law of heat conduction and it states that heat flux is proportionate to the temperature gradient. If the temperature varies in all three directions, equation (7) can be written as,

$$q_x = -k\,\frac{\partial T}{\partial_x} \quad (8)$$

$$q_y = -k\,\frac{\partial T}{\partial_y} \quad (9)$$

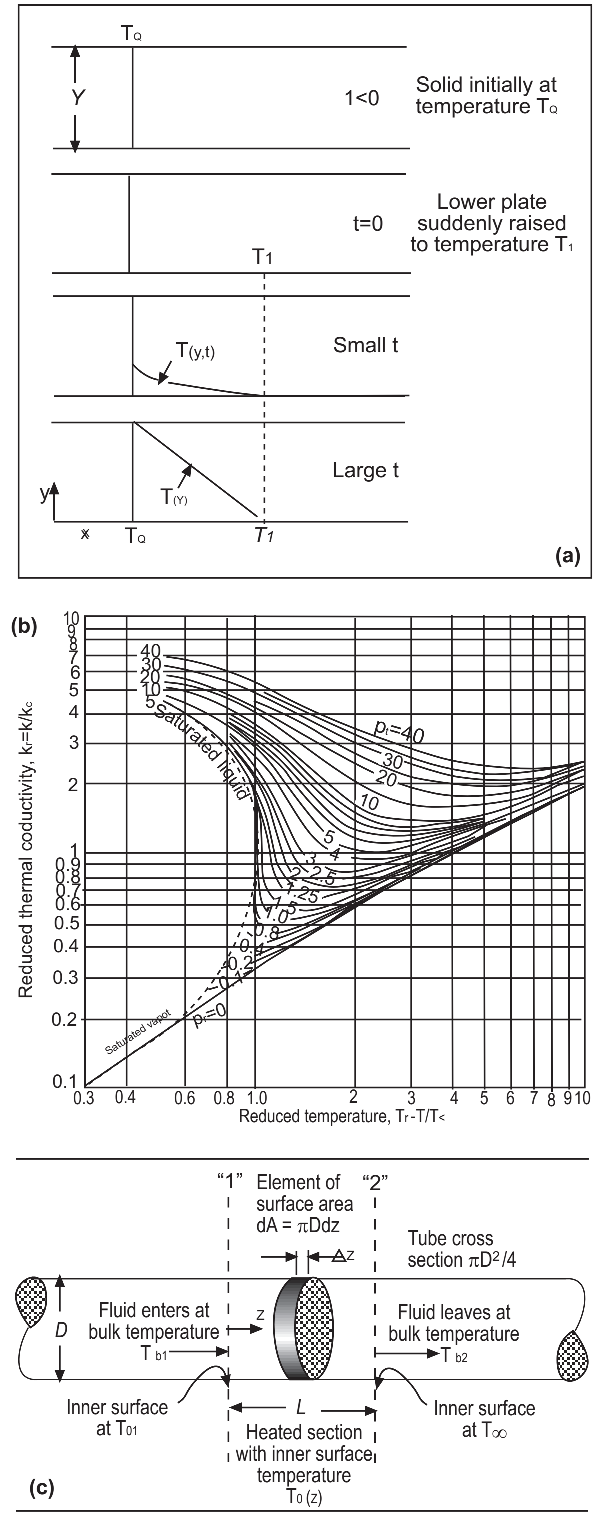


**Fig. 1.** **(a)** Heat transfer through fluid between parallel plates **(b)** Temperature and pressure dependence of thermal **(c)** Heat transfer coefficient estimation.

$$q_z = -k\frac{\partial T}{\partial_z} \quad (10)$$

So, the three-dimensional form of Fourier's law is,

$$q = -k\nabla T \quad (11)$$

A quantity called the thermal diffusivity $\alpha$ is also used. It is defined in equation (12),

$$\alpha = \frac{k}{\rho\hat{C}p} \quad (12)$$

Here $\hat{C}p$ the heat capacity is constant pressure per unit mass. It has the identical dimensions as the kinematic viscosity $\upsilon$ and is often used in related ways in equations of energy transport and momentum change. The ratio $\upsilon/\alpha$ shows the affluence of momentum and energy transfer in flow systems. It is called the Prandtl number and it is as follows (Mohan *et al*., 2017).

$$Pr = \frac{v}{\alpha} = \frac{\hat{C}_p\mu}{k} \quad (13)$$

**Rate of heat addition.** Heat is coming in by faces. At each beginning, have heat flux q. q is a vector quantity. Therefore, it has three components.

$$q = q_x + q_y + q_z \quad (14)$$

$$Q = q.A \quad (15)$$

Q = rate of heat addition; Q = rate of heat flux and A = area

Rate of work done by the forces = F.V

There are two forces involved that are body force and surface forces:

$$F = F_b + F_s \quad (16)$$

In the case of body forces:

$$Fb.\ V = (F_{bx} + F_{by} + F_{bz}).\ (u + v + w) = [\rho g_x u + \rho g_y v + \rho g_z w]\ \Delta x\Delta y\Delta z \quad (17)$$

In the case of surface forces:

$$F_s.\ V = (\text{sum of stresses}).\ \text{area} \quad (18)$$

Two types of stress are normal stress and shear stress; Since $q = -k\Delta T$

$$qx = -\frac{k\partial T}{\partial_x}\ qy = -\frac{k\partial T}{\partial_y}\ qz = -\frac{k\partial T}{\partial_z} \quad (19)$$

From the energy balance equation:

$$-\frac{\partial q_x}{\partial_x} - \frac{\partial q_y}{\partial_y} - \frac{\partial q_z}{\partial_z} = -\frac{\partial}{\partial_x} + \frac{\partial}{\partial_y} + \frac{\partial}{\partial_z}$$

$$(q_x + q_y + q_z) \quad (20)$$

$$-\frac{\partial q_x}{\partial_x} - \frac{\partial q_y}{\partial_y} - \frac{\partial q_z}{\partial_z} = \Delta q \quad (21)$$

$$-\frac{\partial q_x}{\partial_x} - \frac{\partial q_y}{\partial_y} - \frac{\partial q_z}{\partial_z} =$$

$$-\Delta(-k\Delta T) = \Delta(k\Delta T) \quad (22)$$

Also;

$$-u\frac{\partial_p}{\partial_x} - v\frac{\partial_p}{\partial_y} - w\frac{\partial_p}{\partial_z} = \frac{-Dp}{D_t} \quad (23)$$

Also;

$$\frac{\partial}{\partial t}\left[\rho\left\{e + \frac{1}{2}(u^2 + v^2 + w^2)\right\}\right]$$

$$+\frac{\partial}{\partial_x}\left[\rho(e + \frac{1}{2}u^2)\right]$$

$$+\frac{\partial}{\partial_y}\left[\rho(e + \frac{1}{2}v^2)\right]$$

$$+\frac{\partial}{\partial_z}\left[\rho(e + \frac{1}{2}w^2)\right] = \rho\frac{Dh}{Dt} \quad (24)$$

where:

h = specific enthalpy. Thus, the final form of the energy balance is:

$$\rho\frac{Dh}{Dt} = -\frac{Dp}{Dt} + \Delta(k\Delta T) + \varnothing \quad (25)$$

where $\varnothing$ is the viscous.

**Thermal conductivity of temperature and pressure dependence.** If thermal conductivity facts for a compound are not given, it is estimated using the corresponding states chart established on thermal conductivity data for several monatomic substances as shown in Fig. 1b. This chart is a plot of the abridged thermal conductivity $k_r = k/k_c$ which is the thermal conductivity at given conditions divided by the thermal conductivity at the critical point. This $k_r$ is plotted as a purpose of the reduced temperature $T_r = T/T_c$ and the reduced pressure $p_r = p/p_c$. It can be used for the polyatomic substances for the rough estimates of thermal conductivities. It should not be used in near critical conditions (Al-Araji *et al*., 2021; Ahmed *et al*., 2020; Akbar *et al*., 2018, Patil *et al*., 2017).

**Heat transfer coefficient.** Consider a stream framework with the liquid streaming either in a conductor or around a strong article. Assume that warmth is being transported from the solid to the liquid. The heat flow rate across the robust liquid interface would rely upon the interface territory and the temperature drop between the fluid and the strong is appeared in Fig. 1c. The proportionality factor h (the heat transfer coefficient) is defined in equation (26).

$$Q = hA\Delta T \quad \text{......} (26)$$

where:

Q = is the heat flow; A = is the interface area and $\Delta T$ = is the temperature difference. Here h cannot be defined before the area and the temperature drop is specified.

As an example for flow in a conduit, flow through a circular tube is considered. Tube diameter is D and a heated wall division of length L. The tube inside temperature is $T_0(z)$ which varies from $T_{01}$ to $T_{02}$. The bulk temperature of the fluid is $T_b$ that rises from $T_{b1}$ to $T_{b2}$ due to heat. Then three conventional definitions for the heat transfer coefficient are (Jaliliantabar *et al*., 2021; Ijaz *et al*., 2020, Mohan *et al*., 2017).

$$Q = h_1(\pi DL)\,(T_{01} - T_{b1}) = h_1(\pi DL)\Delta T_1 \quad \text{......} (27)$$

$$Q = h_a(\pi DL) = \left(\frac{(T_{01} - T_{b1}) + (T_{02} - T_{b2})}{2}\right) \equiv$$

$$h_a(\pi DL)\Delta T_a \quad \text{......} (28)$$

$$Q = h_{1n}(\pi DL) = \left(\frac{(T_{01} - T_{b1}) - (T_{02} - T_{b2})}{{}_{1n}(T_{01} - T_{b1}) - {}_{1n}(T_{02} - T_{b2})}\right) \equiv$$

$$h_{1n}(\pi DL)\Delta T_{1n} \quad \text{......} (29)$$

where:

$h_1$ = is depends on the expected temperature difference $\Delta T_1$, $h_a$ = is depends on the arithmetic mean $\Delta T_a$ differences in terminal temperature and $h_{1n}$ is established on the logarithmic mean temperature difference $\Delta T_{1n}$, $h_{1n}$ = is preferred during calculations as it is less dependent on L/D. If the properties of fluid change appreciably, then it is better to use the differential form for equation (27).

$$dQ = h_{1OC}(\pi Ddz)\,(T_O\text{-}T_b) = h_{1OC}(\pi Ddz)\Delta T_{1OC} \quad \text{...} (30)$$

Here dQ = is the amount of heat added in distance dz, and subscript $l_{OC}$ corresponds to the local values of h and $\Delta T$, depending on the shape of the element of the area.

For instance for flow around a submerged object, fluid flow around a sphere is considered. The sphere has a radius R and the outer surface is kept up at a temperature $T_O$. Bulk fluid temperature approaching sphere is $T\infty$. The mean heat transfer coefficient $hT_m$ can be defined as:

$$Q = h_m(4\pi R^2)\,(T_O\text{-}T\infty) = \quad \text{......} (31)$$

The local coefficient can also be written as:

$$dQ = h_{lOC}(dA)\,(T_O - T\infty) = \quad \text{......} (32)$$

In heat transfer rate calculations where one or more solid layers separate fluid streams, it is convenient to use the overall heat transfer coefficient, $U_O$ which shows the combined effect of all the resistances through which the heat flows. $U_O$ can be defined in the case of heat transfer between a hot ($T_h$) and a cold ($T_C$) stream separated by a tube of the inner diameter $D_O$ and outer diameter $D_1$.

$$dQ = U_O(\pi D_O dz)\,(T_h\text{-}T_C) \quad \text{......} (33)$$

$$\frac{1}{D_O U_O} = \left(\frac{1}{D_O U_O} + \frac{\ln(D_1/D_2)}{2K_{01}} + \frac{1}{D_1 h_1}\right)_{1OC} = \quad \text{.....} (34)$$

**Nusselt number.** Ease the calculations of thermal conductivity and heat transfer coefficient. A dimensionless factor is introduced called as Nusselt number. It is defined by using thermal conductivity and characteristic diameter:

$$Nu = \frac{hD}{k} \quad (35)$$

Nusselt number based on Prandtl number and Reynolds number in forced convection and Grashof number and Prandtl number in free convection. Nusselt number varies with four dimensionless groups, that is, Nu = Nu(Re,Pr,L/D,$\mu_b/\mu_o$). Here $\mu_b$ is the bulk temperature and $\mu_o$ wall temperature. If density also varies significantly, it carries the condition towards free convection and this variation is considered by including the Grashof number and the relationships. The heat transfer coefficient h is based on eight physical quantities D, ν, ρ, $\mu_b$, $\mu_o$, $\hat{C}pk$, L, while Nu initially depends on just four dimensionless quantities. So, calculating Nu and then going for h saves much time and effort (Alqahtani *et al*., 2020, Goudarzi *et al*., 2020).

**Turbulence modeling.** Turbulence representative is the enlargement and usage of a scientific model to anticipate the effects of choppiness. Fierce streams are ordinary in most unaffected circumstances. Regardless of many years of research, there is no systematic hypothesis to predict these passionate streams advancement. The conditions administering fierce streams must be illuminated legitimately for specific instances of the stream. For most authentic furious streams, CFD recreation uses Fierce models to anticipate the improvement of unsettling influence. These choppiness models are streamlined constitutive situations that predict the substantial growth of violent streams.

K-Epsilon (k-ε) turbulence model is generally a superficial model utilized in computational fluid components (CFD) to impersonate mean stream credits for savage stream conditions. It is a two condition model that depicts fracas by methods for two vehicle conditions (PDEs). The first driving force for the K-epsilon model was to enhance the blending length model to find a choice to mathematically support approving fierce scales in adequate to highly complex nature streams. Like earlier turbulence models, the k-ε model bright lights on the instruments that impact the savage engine imperativeness. The blending length model misses the mark on such a consensus. This model's critical assumption is that the thickness is isotropic by the days end, the extent between Reynolds stress and the mean pace of miss happening is comparable all over.

The specific k-ε equations contain numerous incomprehensible and immense expressions. For a substantially more functional methodology the standard k-ε turbulence model, hence limiting questions and leading many conditions to be functional to numerous fierce applications (Al-Araji *et al*., 2021; Abhilash *et al*., 2021, Akbar *et al*., 2018, Patil *et al*., 2017). For turbulent kinetic energy k:

$$\frac{\partial(\rho_k)}{\partial_t} + \frac{\partial(\rho_{kui})}{\partial_{xi}} = \frac{\partial}{\partial_{xj}}\left(\frac{\mu_t}{\sigma_k}\frac{\partial_k}{\partial_{xj}}\right) + $$

$$+ 2\mu_t E_{ij} E_{ij} - \rho\varepsilon \quad (36)$$

For dissipation:

$$\frac{\partial(\rho\varepsilon)}{\partial_t} + \frac{\partial(\rho\varepsilon_{ui})}{\partial_x} = \frac{\partial}{\partial_{xj}}\left(\frac{\mu_t}{\sigma\varepsilon}\frac{\partial\varepsilon}{\partial_{xj}}\right) + $$

$$C_{1\varepsilon}\frac{\varepsilon}{k} 2\mu_t E_{ij} E_{ij} - C_{2\varepsilon}\,\rho\,\frac{\varepsilon^2}{k} \quad (37)$$

The Navier-Stokes equations are insightful conditions. If need to settle them by PC, need to move them into the discretized structure this cycle is discretization. The ordinary discretization strategies are limited distinction, limited component and limited volume techniques. Here present the limited volume strategy.

**Finite volume method.** The finite volume strategy utilizes the essential type of preservation conditions as its beginning stage. The arrangement space is subdivided into a limited number of adjacent control volumes (CVs) and the protection conditions are connected to every control volume. At the centroid of every control volume lies a computational hub at which the variable qualities are determined. Insertion is utilized to express factor esteems at the control volume surface as far as the nodal (control volume focus) values. Surface and volume integrals are estimated using reasonable quadrature formulae. Therefore, one acquires an arithmetical condition for every control volume, where various neighbor nodal qualities show up.

The FV technique can oblige any sort of framework, so it is reasonable for intricate geometries. The lattice characterizes just the volume control limits and need not be identified with an arranged framework. The strategy is moderate by development, in as much as surface integrals (diffusive and convective transitions) is the equivalent for the control volumes sharing limit. The finite volume approach is maybe the least difficult to comprehend and program. All relationships that need to be approached have physical importance, so it is well known to specialists. FV techniques' weakness contrasted with FD plans is that strategies for requests higher than a second are progressively hard to create in 3D. The finite volume methodology involves three degrees of estimate: addition, separation, and coordination (Awais *et al*., 2020; Kocheril and Elias, 2020, Akbar *et al*., 2018; Mohan *et al*., 2017).

**Basic steps in finite volume method.** For separation, the ceaseless area into various distinct subdomains by a lattice. The network characterizes the limits of a CV. For each sub-area, get overseeing logarithmic conditions from the administering differential conditions. Acquire an arrangement of algebraic equations. Understand the above structure of logarithmic conditions to acquire the reliant factors' estimations at recognized discrete focuses (computational hubs) (Subhedar *et al*., 2018; Goudarzi and Jamali, 2017).

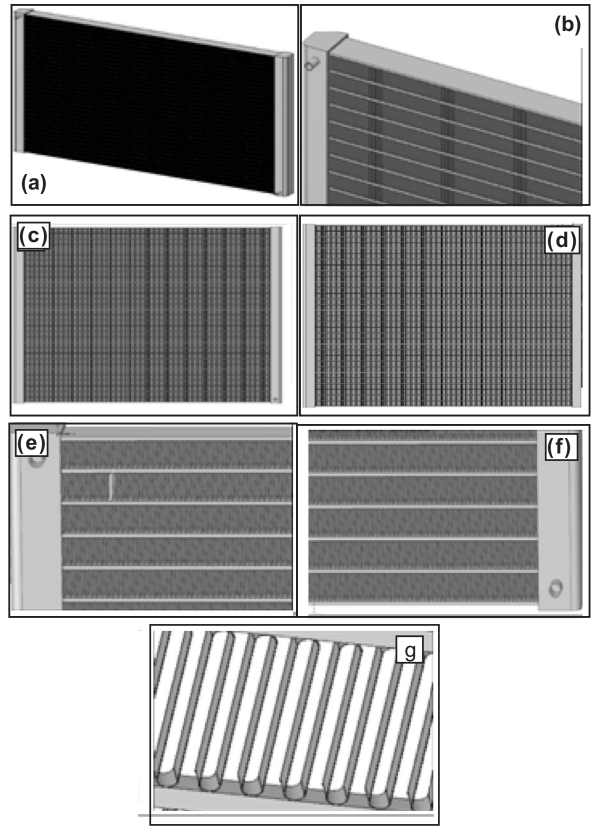


**Fig. 2.** **(a)** Complete radiator **(b)** Close-up view of radiator **(c)** Front view **(d)** Rear view **(e)** Coolant outlet **(f)** Coolant inlet **(g)** Wavy fins.

## Result and Discussion

**Model 1 simulation.** ANSYS is a generally helpful limited component exhibiting bundle for mathematically solving a wide variety of mechanical issues. These problems include structural study (linear and nonlinear) and fluid problems, heat transfer, static/dynamic, acoustic and electromagnetic issues. This study uses a design modeler (the default designing tool of ANSYS) or ANSYS space claim to design any ANSYS equipment. For creating the car radiator which is used ANSYS space claim because it is facile to use. The design modeler is relatively arduous because you have to select the plane manually one by one but in space claim, with one click, you can change the plane and can work on it. It can easily edit a shape in space claim. Space claim can translate, open and edit any CAD file from any powerful CAD tool.

To select any part of the geometry, if you want to choose a different plane, you click sketch mode and then change the plane by selecting the object's working face. Select faces to revolve, sweep, scale or copy. It can also extrude the body using pull. To view all the faces of the geometry may rotate the body using spin. This is to shift it at any place on the design window and also used to enlarge or reduce the geometry. It also has a zoom inbox option used to target the face or edge that is used to be observed and enlarge it. It is used to drag the object or make multiple copies of the geometry. It is also used to change the orientation of the geometry. It can also change dimensions by clicking the space bar, while selecting an axis or edge. The combine is used to merge or split two bodies and also to align the components by selected axes, points or planes. In detail, you have a dimension tool that is used to display the dimensions of the geometry.

**Specifications and designing of the radiator.** The specifications of the radiator have taken from the article for Maple soft software for radiator design. Tube shape = Rectangular; Fin shape = Wavy; radiator length ($r_L$) = 457.2 mm; Radiator width ($r_W$) = 431.771 mm; Radiator height ($r_H$) = 24.6063 mm; Tube width ($t_w$) = 24.6063 mm; Tube height ($t_H$) = 1.56261 mm; Tube length ($t_L$) = 457.2 mm; Fin width ($f_W$) = 24.6063 mm; Fin height ($f_H$) = 11.8813; Fin thickness ($f_T$) = 0.0254 mm; Radius of the curve in fins = 0.523 mm; Fin spacing = 1.046 mm; Number of tubes = 33; Number of fins = 417 and Length of one fin = 1.09 mm.

The radiator has a flat tube because, in circular fluid, the middle fluid does not contact the air. So, the heat transfer rate is decreased but in a flat tube, all layers reach the air and thus enhance heat transfer. This radiator's material is aluminum alloy because aluminum has a greater heat transfer rate and the objective of this research is to improve the heat transfer as shown in Fig. 2a and b). Light weight is also the reason that aluminum is used as the material for the radiator. Secondly, this type of radiator is also being used by various companies like Jainsu Unbeatable Energy Group Company (China) (Akbar *et al*., 2018; Patil *et al*., 2017).

It uses fins in our radiator because fins enhance increases the contact area of the tube and thereby improving the convection of coolant within, as shown in Fig. (2c, d, e and f). They considered wavy fins because it improves the heat transfer influence to a higher degree than corrugated fins. They also provide the best output to air pressure drop ratio. The default fin shape is wavy if not specified as shown in Fig. 2g.

**Designing of control volume.** In thermodynamics and fluid mechanics, the CV is a volume fixed in space or moving with constant velocity (no acceleration), as shown in Fig. 3a. It could be gas or liquid (fluid) flows. They considered a control volume of the tube in which the flow of the coolant is fully developed and turbulent. Initially, designed a control volume consisting of a 40 mm one tube and fins above and below it. The solutions were not satisfactory, so the final control volume was designed using a fully developed flow approach and taking the air heat transfer coefficient constant. Tube length ($t_L$) = 70 mm; Tube width ($t_W$) = 24.6063 mm; Tube height ($t_H$) = 1.56261 mm; Tube thickness ($t_T$) = 0.254 mm.

The radiator's whole geometry could not be solved on the laptop for this needs super computers of high configuration. They considered two fins and one tube for our radiator but the mesh could not be generated. The properties of water and air were taken at 358 K and calculations were made for the respective hydraulic diameters. The turbulent flow model's entrance length was calculated so that the appropriate size of control volume can be considered. The entrance length of turbulance is 7.22 mm.

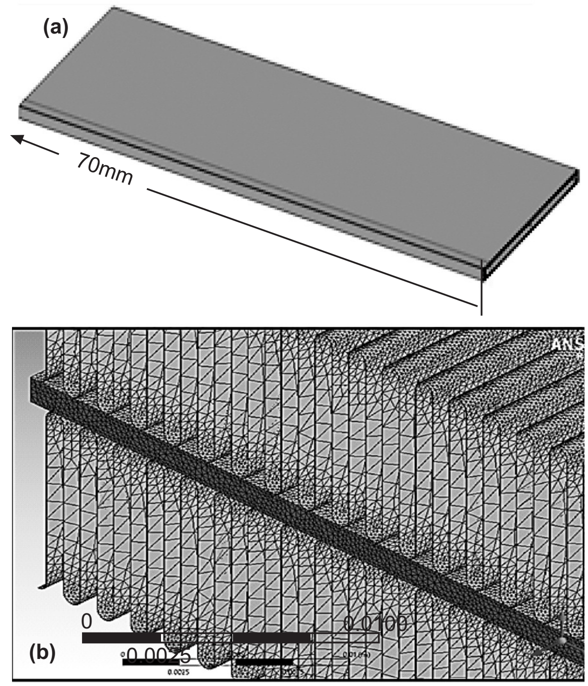


**Fig. 3.** **(a)** Reduced tube as control volume of Model 1 **(b)** Meshed model (2 fins one tube).

**Meshing.** For simulation, the geometry is needed to have meshed. Meshing is dividing the geometry into small parts and dividing it into the form of a tiny cell as shown in Fig. 3b. This mesh may be of several types tetra hederal, triangular mesh, or hexagonal. In some models, the mesh is applied through a specific method because a solution must be performed on refined meshes. Standard methods in ANSYS for refining or applying mesh as follows: refined mesh, inflation and face mesh.

**Simulation and solution.** After meshing, the software moves to the simulation environment where some inputs are required material and its properties, boundary conditions, solution methods, model selection and convergence criteria to set the convergence criteria of

1e⁻⁶. The most critical and challenging step in the simulation is the convergence of equations. In the simulation, the K-epsilon method has been chosen in which two equations, energy and momentum equations, are unraveled in simulation. Sometimes the equations are not quickly converged and a lot of practice is required for convergence. For this purpose simulations were performed on small models for convergence practice. A simple tube was modeled for this purpose. A momentum and energy equation were converged. Figure 4a, b, c, d & e) are shown different results.

**Simulation of selected models.** Figure 5 (a, b & c) shows the solution using two fins and one tube (40 mm).

The Boolean operation (solution using Boolean approach 70 mm) involves combining the two geometric entities. In this, first, subtracted the tube and the coolant part and put the conditions of the air and then preserved the tube as presented in Fig. 6(a, b, c, d & e).

The all tries made, no successful or satisfactory results were obtained from this model due to the unavailability of proper and complete boundary conditions and data.

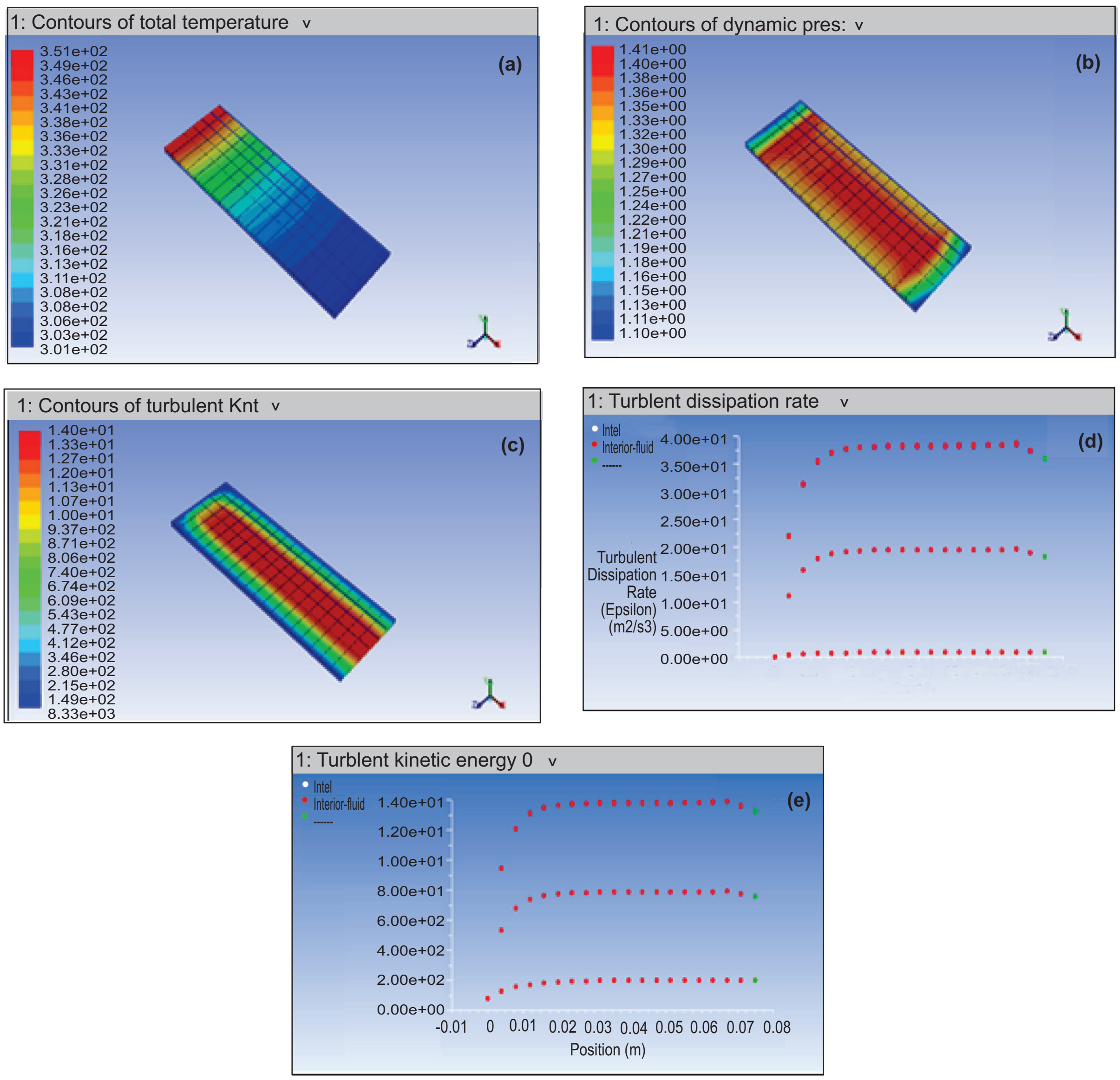


**Fig. 4.** A simple tube of **(a)** Total temperature contours **(b)** Dynamic pressure contours, **(c)** Turbulent kinetic energy contours, **(d)** Turbulent dissipation energy and **(e)** Turbulent kinetic energy.

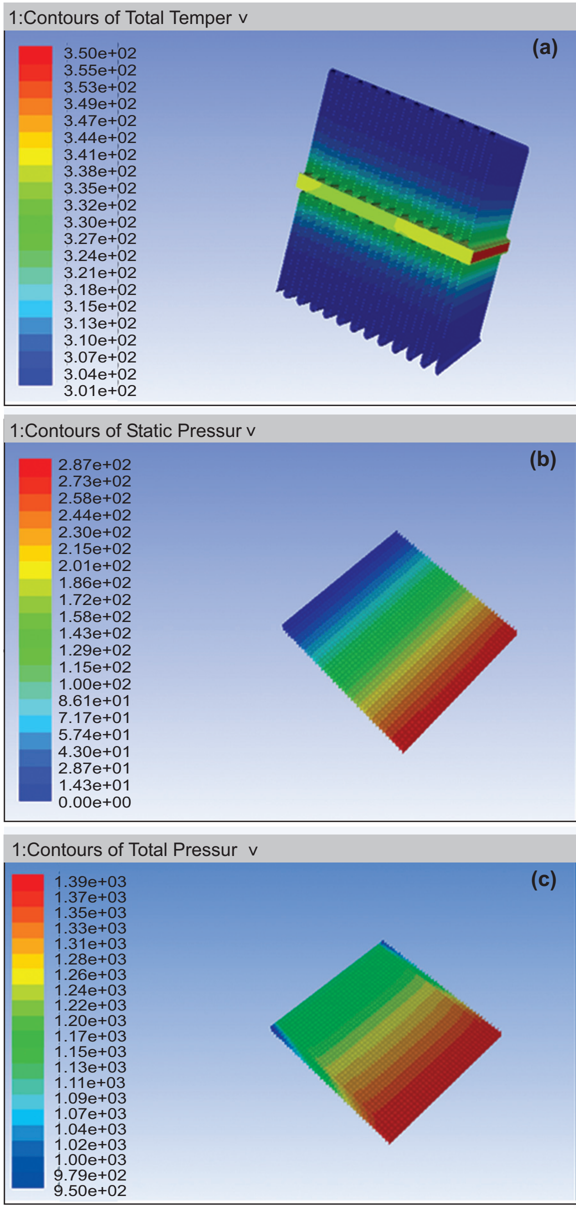


**Fig. 5.** Two fin one tube **(a)** Total temperature contours **(b)** Static pressure contours **(c)** Total pressure contours.

So researched another article and followed its boundary conditions and radiator model for the simulation.

**Model 2 simulation.** Specifications and designing of the radiator tube, Tube width ($t_W$) = 20 mm; Tube height ($t_H$) = 3 mm; Tube length ($t_L$) = 310 mm and Tube radius of curvature = 1.5 mm. Numerical calculations were made for water and ethylene glycol in both pure form and nanoparticle suspension. Purified water was flowing in a turbulent region. In comparison, EG has a laminar flow regime. The properties of water and EG were taken at 40 °C. The properties of nanoparticles were also taken from different experimental data. Tables 3 show the physical properties and Table 4 boundary conditions of various fluids and nanoparticles (Erdoðan *et al*., 2020; Goudarzi and Jamali, 2017; Mohan *et al*., 2017).

The air heat transfer coefficient was assumed to be a constant 150 W/m²/K.

**Boundary conditions for ethylene glycol.** The air heat transfer coefficient was assumed to be a constant 150 W/m²/K. Nanofluids are entered at the same boundary conditions as pure water or pure EG. Those correlations are given below:

$$\mu nf = \mu bf + \frac{\rho p * VB * dp^2}{72 * C * S} \text{ (Viscosity) .......... (38)}$$

$$\kappa nf = \frac{\kappa p+(\Phi-1)kbf-\varphi(\Phi-1)\,(kbf-kp)}{kp+(\Phi-1)kbf+\varphi(kbf-kp)} * kbf \text{ (Conductivity) ... (39)}$$

**Table 4.** Boundary conditions for pure water simulation

| Flow regime | Turbulent | |
|---|---|---|
| | Water | Ethylene glycol |
| Reynolds number | 10000-30000 | 1000-3000 |
| Inlet velocity (m/s) | 1.18-3.37 | 1.36-3.17 |
| Tube inlet temperature (°C) | 40 | 40 |
| Air inlet temperature (°C) | 30 | 30 |

**Table 3.** Physical properties at 40 °C

| Properties | Water | Ethylene glycol | Nano Particles $Al_2O_3$ |
|---|---|---|---|
| Density (Kg/m³) | 990.2 | 994.241 | |
| Viscosity (Kg/m/s) | 0.000596 | 0.000928 | - |
| Thermal conductivity (W/m/K) | 0.64 | 0.24 | 36 |
| Specific heat (J/Kg/K) | 4180 | 2470 | 880 |
| Size | - | 20 nm | |
| Empirical shape factor (Φ) | - | | 3 |

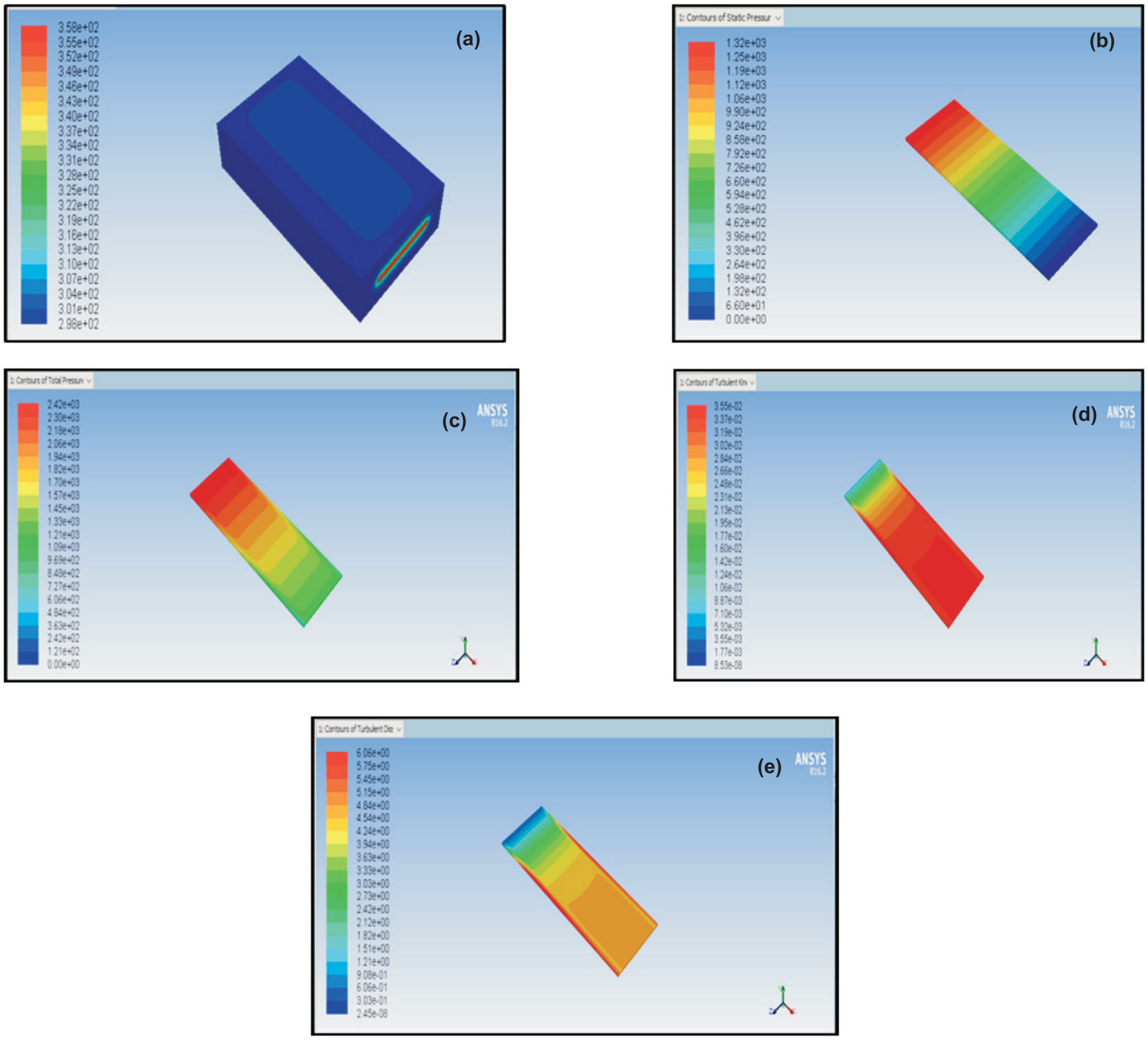


**Fig. 6.** Boolean approach contours **(a)** Total temperature **(b)** Static pressure **(c)** Total pressure **(d)** Turbulent kinetic energy **(e)** Turbulent dissipation energy.

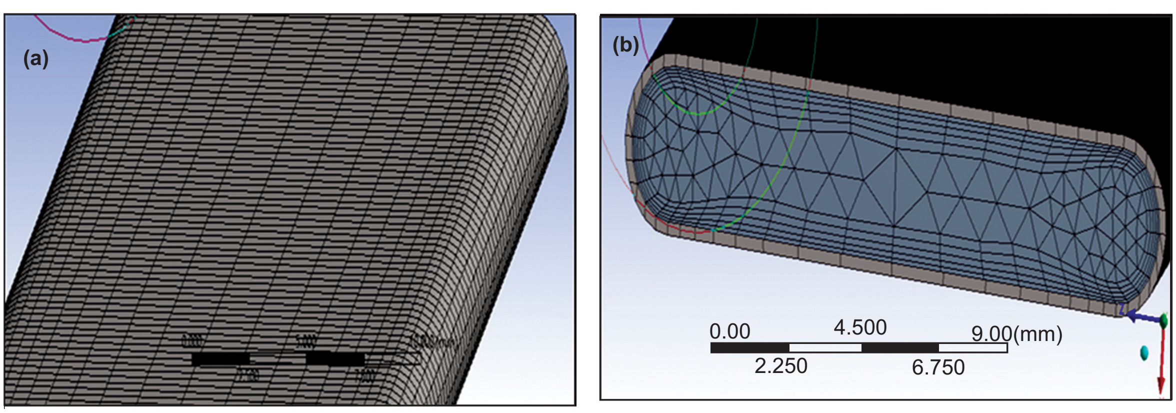


**Fig. 7.** **(a)** Rough tetrahedral mesh **(b)** Refined triangular mesh.

$$\rho nf = \varphi \rho p + (1\text{-}\varphi)\ \rho bf \quad \text{(Density)} \ ................ \ (40)$$

$$Cpnf = \frac{\varphi \rho p Cpp + (1 - \varphi)\ \rho bf Cpbf}{Pnf} \quad \text{(Specific heat)} \ ... \ (41)$$

**Meshing.** After refining the model, the triangular mesh is presented in Fig. 7(a & b). The statistics of mesh metric is none, nodes 226948 and elements are 461191.

Pure water contours shown in Fig. 8(a, b, c, d, e & f).

Pure ethylene glycol contours are shown in Fig. 9(a, b, c & d).

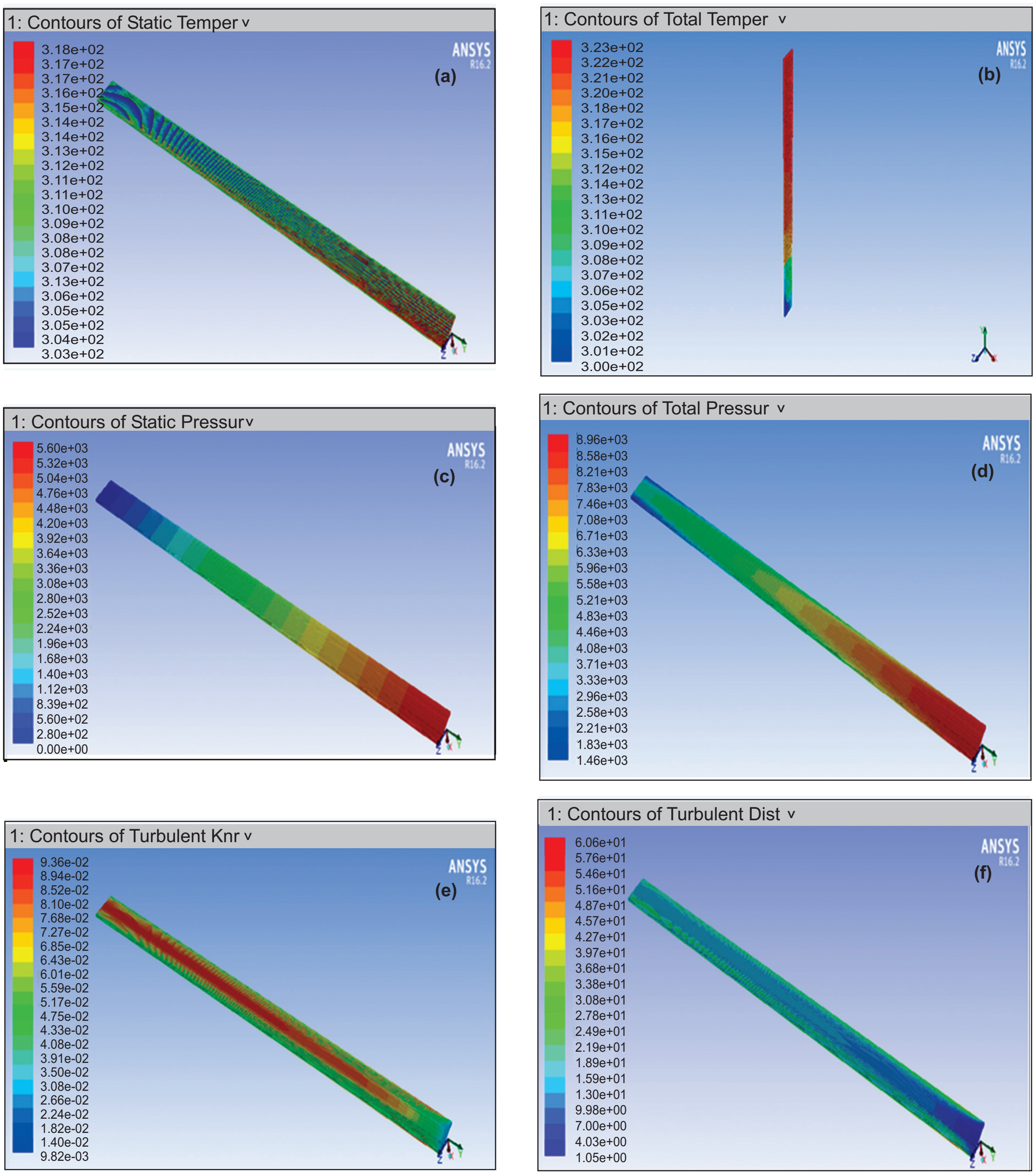


**Fig. 8.** Water **(a)** Static temperature contour **(b)** Total temperature contour **(c)** Static pressure contour **(d)** Total pressure contour **(e)** Turbulent kinetic energy contour **(f)** Turbulent dissipation energy contour.

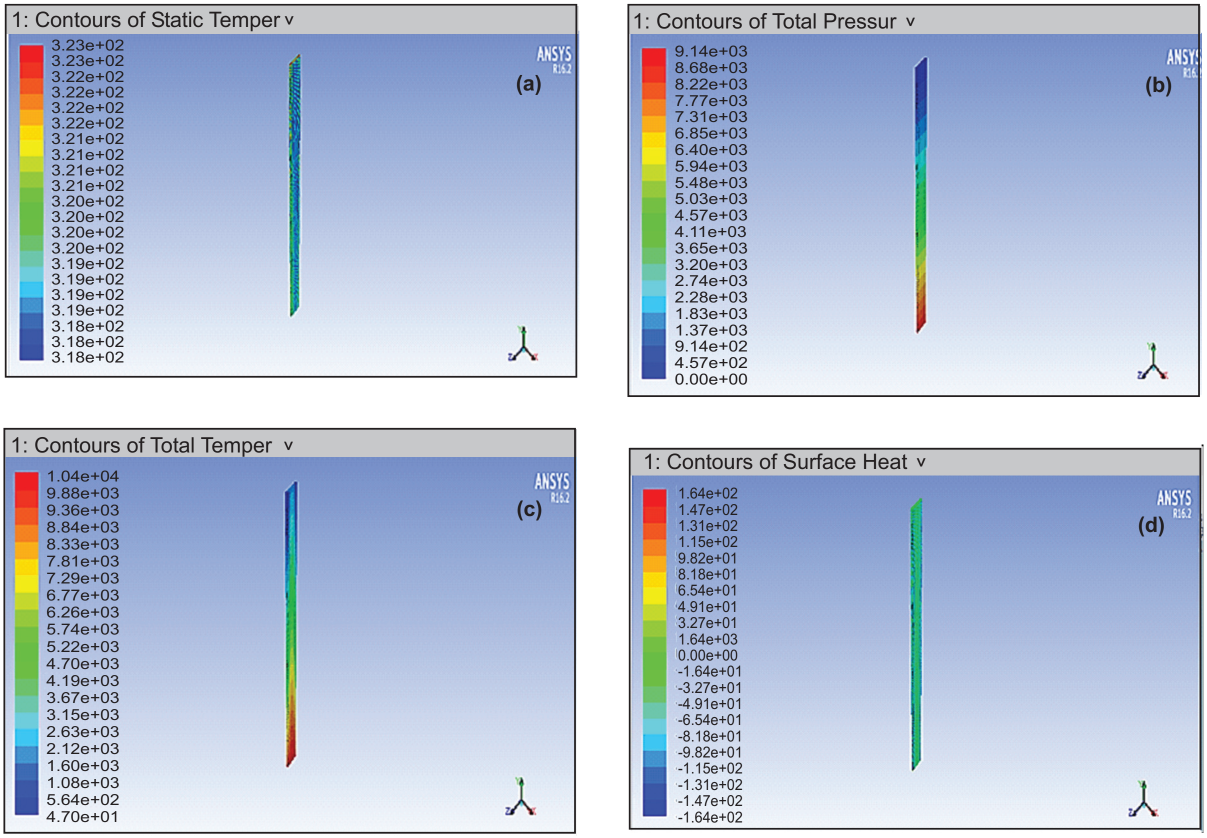


**Fig. 9.** Ethylene glycol **(a)** Static temperature contour **(b)** Static pressure contour **(c)** Total pressure contour **(d)** Surface heat contour.

Water-based nanofluid contours without creating a database are presented in Figure 10 (a, b, c, d, e & f).

**Database for Nano-particles $Al_2O_3$ and water-based.** ANSYS has its database for the properties of the material and is selected like other software. These databases are still limited or can say that standard materials are present in their database. Nanoparticle based material has different properties which are calculated by using various correlations. For simulation purposes, these properties are to be entered into the software manually by the user. A user-defined database may be created as shown in Fig. 11(a & b) (Nagib *et al*., 2019; Reddy *et al*., 2019; Patil *et al*., 2017).

Figure 12 (a, b, c, d, e & f) shows the water-based nanofluid contours after creating a database.

**Pure water excel versus simulation.** A comparative study was carried out based on calculated and simulated results. Nusselt number calculations were performed by using suitable correlations and compared the results with CFD simulation.

Figure 13(a) shows the CFD results comparison with the numerical solution for the Nusselt number of pure water. Two correlations, Dittus boater and Gnelski were used and it was found that the CFD results were close to the dittuus Boelter. It means that the designed model is valid on the Dittus Boelter correlation. The same work was performed on the EG system using the Vajha correlation and compared with the CFD results. Figure 13(b) shows that by increasing the Reynolds number, the error between CFD and numerical results increased. The nanofluid results are shown in Table 5 (Li *et al*., 2021; Mandole *et al*., 2020; Karimi and Afrand, 2018).

The effect of different concentrations of nanoparticles in base fluid on Nusselt number was also studied. It is found that the higher the concentration of nanoparticles in base fluid higher the Nusselt number was found.

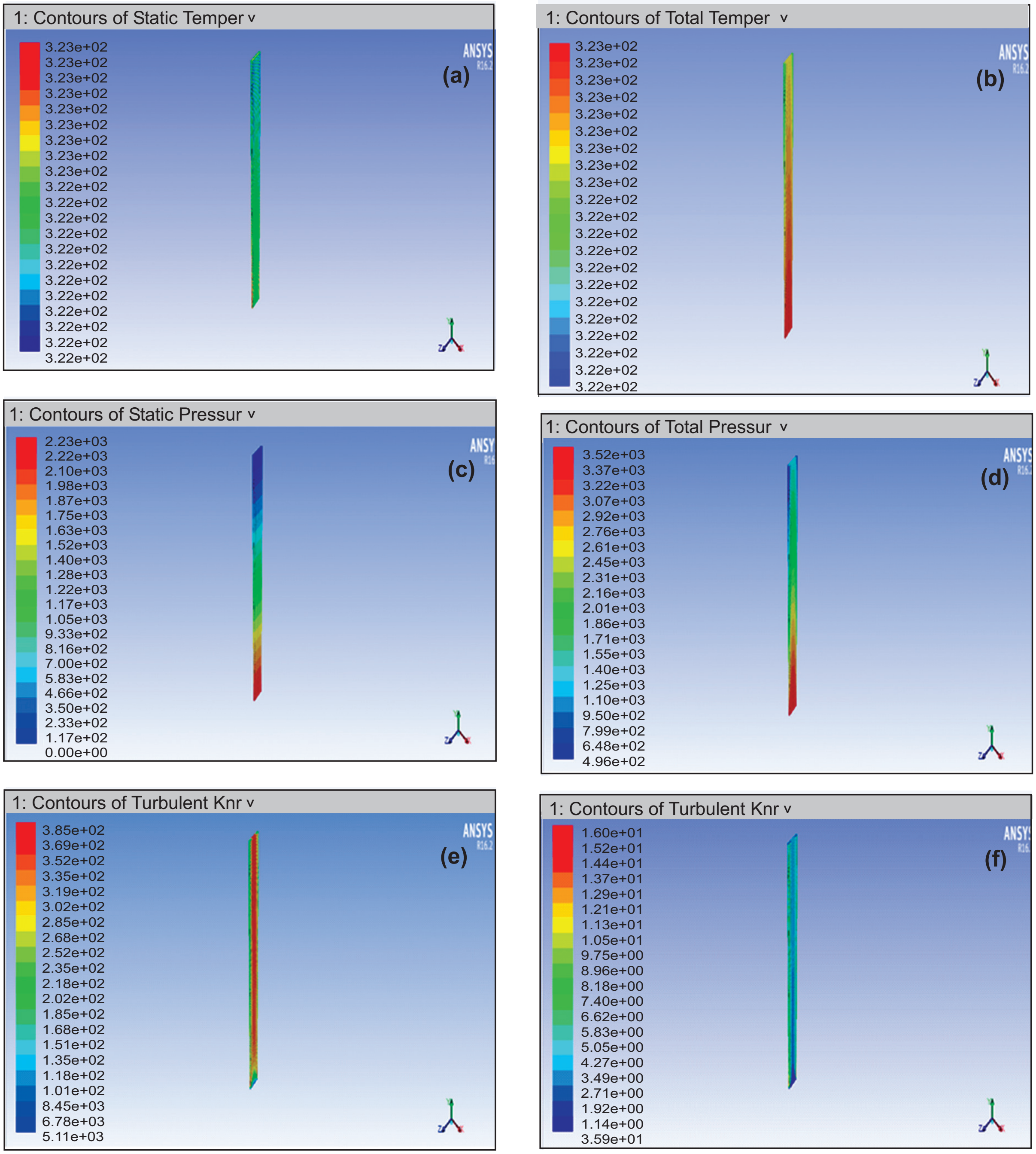


**Fig. 10.** Water-based nanofluid without database **(a)** Static temperature contour **(b)** Total temperature contour **(c)** Static pressure contour **(d)** Total pressure contour **(e)** Turbulent kinetic energy contour **(f)** Turbulent dissipation energy contour.

Figure 14(a) shows the result of water based alumina particles nanofluid. The same results were obtained for the EG-based alumina nanoparticles fluid as shown in Fig. 14(b).

The effect of different boundary conditions on the Nusselt number was observed by changing the coolant's inlet flow. A higher flow rate resulted from a higher Nusselt number. Figure 15(a) shows the result for water based nanofluid. The same analysis was carried out for EG-based nanofluid. The results were also the same in

```
;;;;;;;;;;;;;;;;;;;;;;;;;;;;;;;;;;;;;;;;;;;;;;;;;;;;;;;;;;;;;;;;;;;;;;;;;;;;;;;;
;;;          Fluent USER DEFINED MATERIAL DATABASE                          ;;;
;;;                                                                         ;;;
;;;   (name type [fluid/solid] (chemical - formula . formula)               ;;;
;;;   (prop1 (method1a . data1a) (method1b . data1b))                       ;;;
;;;   (prop2 (method2a . dat2a) (method2b . data2b)))                       ;;;
;;;;;;;;;;;;;;;;;;;;;;;;;;;;;;;;;;;;;;;;;;;;;;;;;;;;;;;;;;;;;;;;;;;;;;;;;;;;;;;;

(fluid-1 fluid)
      (chemical-formula . #f)
      (density (constant . 4000.))
      (specific-heat (conant. 880.))
      (therma1-conductivity (constant . 35.))
```

```
;;;;;;;;;;;;;;;;;;;;;;;;;;;;;;;;;;;;;;;;;;;;;;;;;;;;;;;;;;;;;;;;;;;;;;;;;;;;;;;;
;;;          Fluent USER DEFINED MATERIAL DATABASE                          ;;;
;;;                                                                         ;;;
;;;   (name type [fluid/solid] (chemical - formula . formula)               ;;;
;;;   (prop1 (method1a . data1a) (method1b . data1b))                       ;;;
;;;   (prop2 (method2a . dat2a) (method2b . data2b)))                       ;;;
;;;;;;;;;;;;;;;;;;;;;;;;;;;;;;;;;;;;;;;;;;;;;;;;;;;;;;;;;;;;;;;;;;;;;;;;;;;;;;;;
(fluid-1 fluid)
   (chemical-formula . #f)                       (water_liquidcH20> . #f
   (density (constant . 4000.))                  (specific-heat (constant . 4182))
   (specific-heat (conant. 880.))                (density (constant . 998.2 ))
   (therma1-conductivity (constant . 35.))       (thermal - conductivity (consant . 0.6))
   (volumetric concentration (constant .1 ))     (viscosity (costant . 0.001003))
```

**Fig. 11.** Database for **(a)** $Al_2O_3$ **(b)** Water-based $Al_2O_3$ nano-fluid.

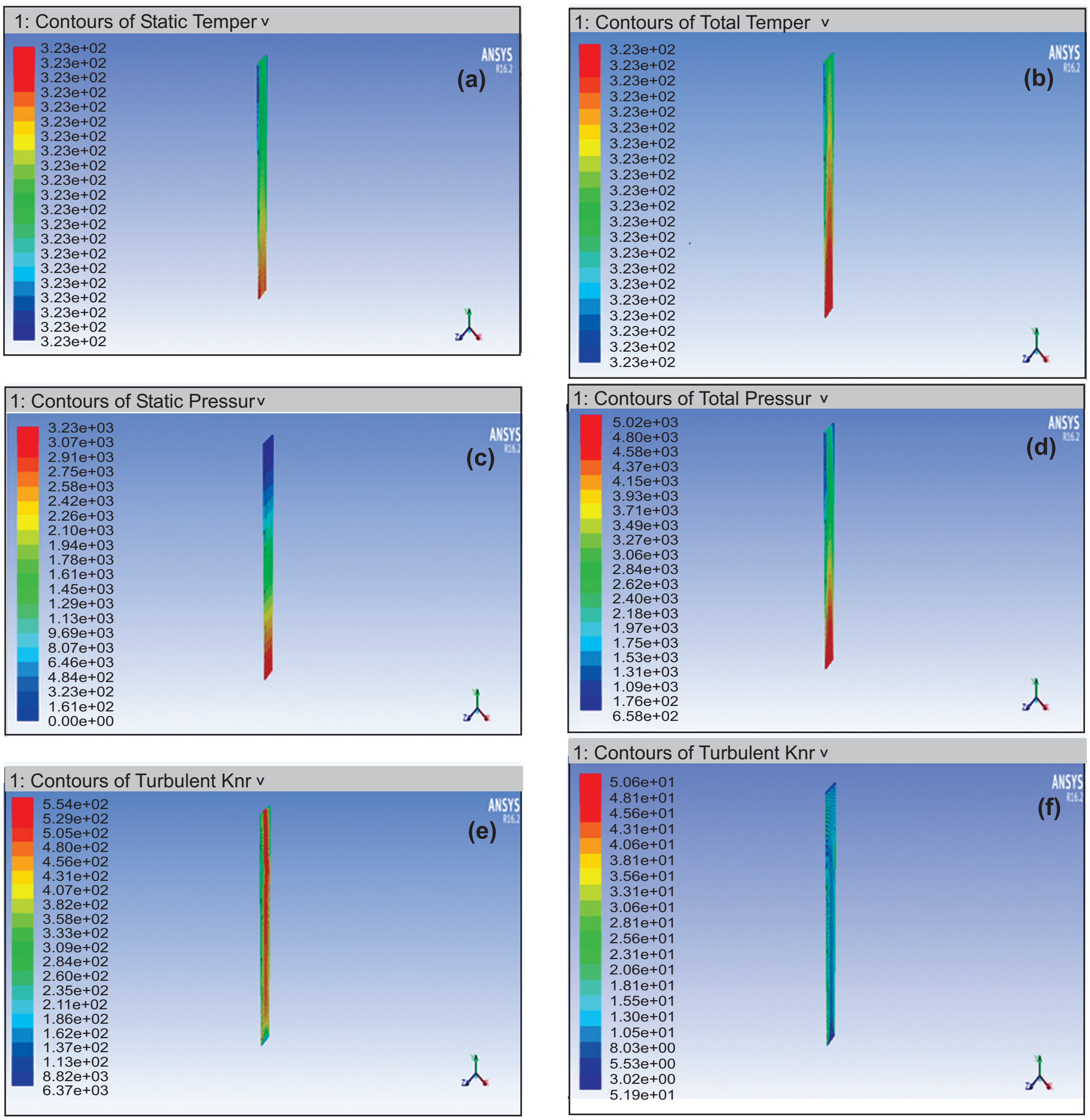


**Fig. 12.** Water-based nanofluid with database contour **(a)** Static temperature **(b)** Total temperature **(c)** Static pressure **(d)** Total pressure **(e)** Turbulent kinetic energy **(f)** Turbulent dissipation energy.

**Table 5.** Nanofluid results

| $Al_2O_3$ water based nanofluid with inlet temperature of 40 °C | | | | | $Al_2O_3$ EG based nanofluid with inlet temperature of 40 °C | | | | |
|---|---|---|---|---|---|---|---|---|---|
| Conc.(%) | Re | Ve | Nu | Pr | Conc.(%) | Re | Ve | Nu | Pr |
| 1 | 10000 | 1.09208 | 62.89661 | 3.6668075 | 1 | 10000 | 1.693783 | 6.64E+01 | 91.742330 |
| | 20000 | 2.18417 | 109.5094 | 3.6668075 | | 20000 | 3.387566 | 8.80E+01 | 91.742330 |
| | 30000 | 3.27625 | 151.4692 | 3.6668075 | | 30000 | 5.081349 | 1.04E+02 | 91.742330 |
| 1.5 | 10000 | 1.27123 | 66.44171 | 4.2055423 | 1.5 | 10000 | 1.69987 | 6.78E+01 | 91.595015 |
| | 20000 | 2.54245 | 115.6817 | 4.2055423 | | 20000 | 3.399741 | 8.95E+01 | 91.595015 |
| | 30000 | 3.81368 | 160.0066 | 4.2055423 | | 30000 | 5.099611 | 1.05E+02 | 91.595015 |
| 2.5 | 10000 | 1.35639 | 67.3892 | 4.3570814 | 2.5 | 10000 | 1.814678 | 6.93E+01 | 96.774364 |
| | 20000 | 2.71278 | 117.3314 | 4.3570814 | | 20000 | 3.629357 | 9.15E+01 | 96.774364 |
| | 30000 | 4.06917 | 162.2883 | 4.3570814 | | 30000 | 5.444035 | 1.08E+02 | 96.774364 |
| 3.5 | 10000 | 1.56657 | 70.55717 | 4.8873439 | 3.5 | 10000 | 2.094954 | 7.31E+01 | 110.57610 |
| | 20000 | 3.13314 | 122.8472 | 4.8873439 | | 20000 | 4.189909 | 9.65E+01 | 110.57610 |
| | 30000 | 4.69971 | 169.9175 | 4.8873439 | | 30000 | 6.284863 | 1.13E+02 | 110.57610 |
| 4 | 10000 | 1.85172 | 75.00116 | 5.6936382 | 4 | 10000 | 2.470986 | 7.80E+01 | 129.75609 |
| | 20000 | 3.70343 | 130.5846 | 5.6936382 | | 20000 | 4.941971 | 1.03E+02 | 129.75609 |
| | 30000 | 5.55515 | 180.6196 | 5.6936382 | | 30000 | 7.412957 | 1.21E+02 | 129.75609 |

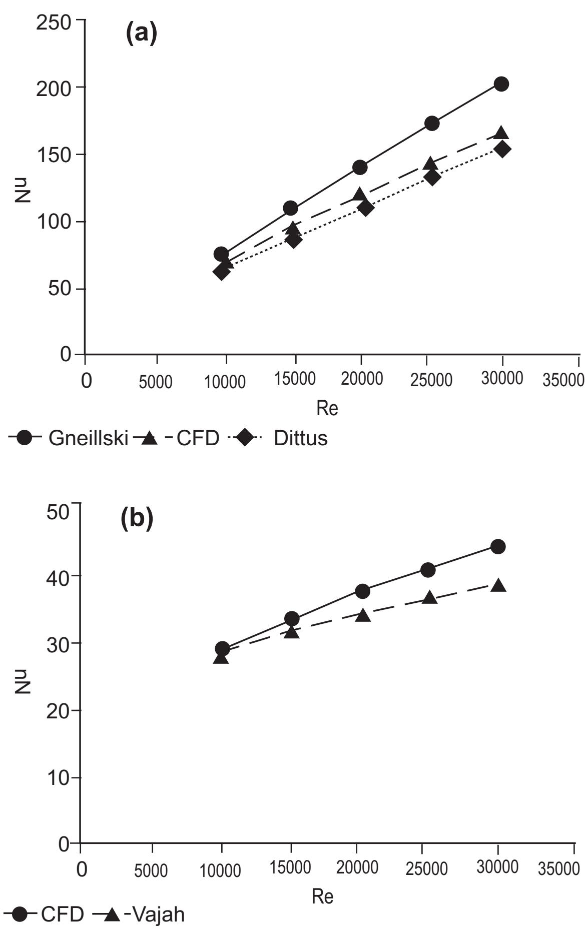


**Fig. 13.** Comparison of numerical results with simulation results inlet temperature 40 °C **(a)** Water **(b)** Ethylene glycol.

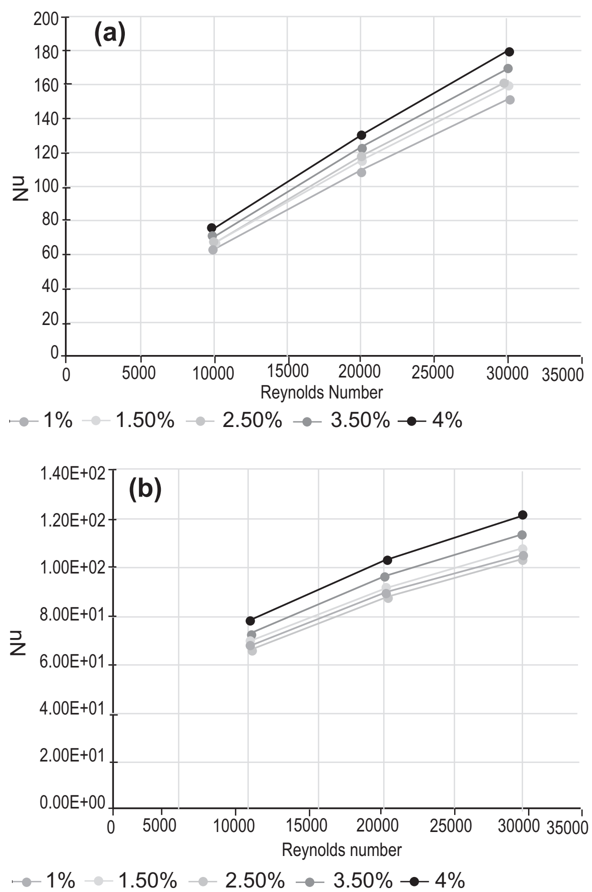


**Fig. 14.** Effect of concentration of nanoparticles on Nusselt number at constant Reynolds number and inlet temperature 40 °C nanofluid **(a)** Water-based $Al_2O_3$ **(b)** ethylene glycol-based $Al_2O_3$.

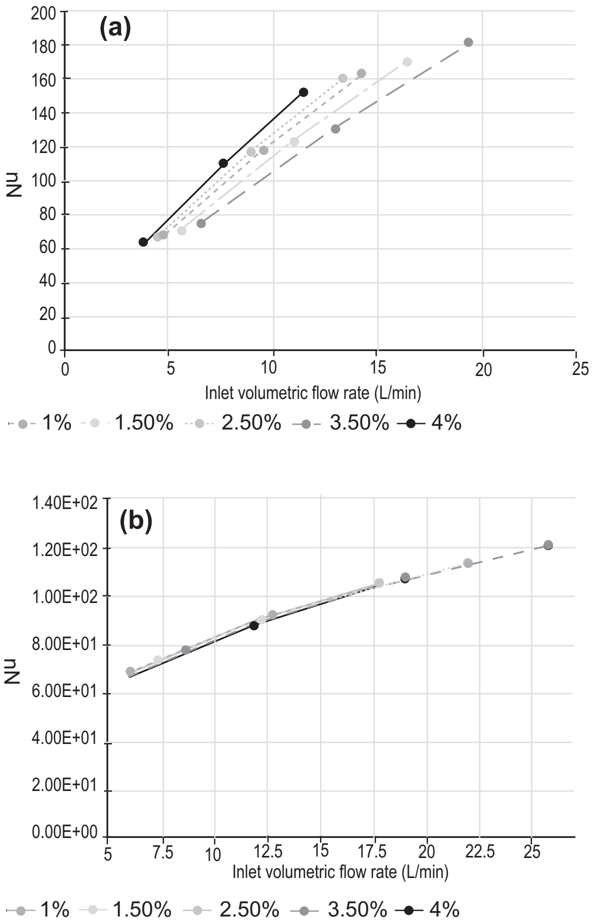


**Fig. 15.** Effect of inlet volumetric flow rate on Nusselt number on different concentrations and inlet temperature is 40 °C nanofluid **(a)** Water-based $Al_2O_3$ **(b)** ethylene glycol-based $Al_2O_3$.

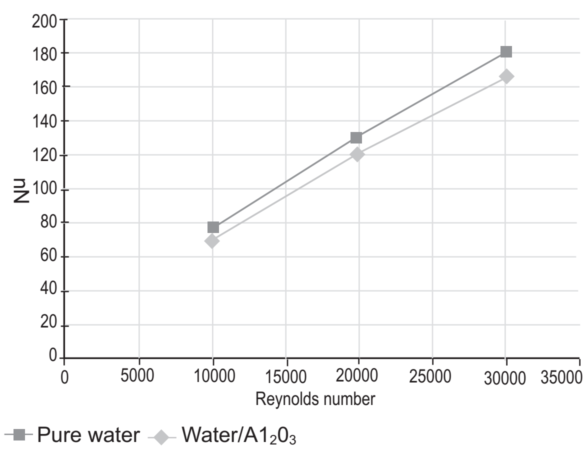


**Fig. 16.** Comparison of Nusselt numbers of pure water and water-based nanofluid.

this case but it may say that there was not much variation but it is observed that the Nusselt number increased, although not to a very large extent. Figure 15(b) shows the result for EG based nanofluid. Figure 16 compares Nusselt numbers of pure water and water based nanofluid (Abhilash *et al*., 2021; Jaliliantabar *et al*., 2021; Mert *et al*., 2021; Goudarzi *et al*., 2020; Mandole *et al*., 2020; Kumar and Krishna, 2017; Patel *et al*., 2017).

## Conclusion

Heating in car radiators is now a day the most challenging problem. Due to the combustion of hot gases, a large amount of heat is produced in the engine head. The engine cools down water has been used for a long as a coolant in standard automobiles. Due to the lower conductivity of pure water coolants other than pure water are being used. The mixer of water with ethylene glycol or other fluids is being used. When the thermal conductivity is taken into account, nanofluids are the one which is being discussed. Nanoparticles have more significant conductivity due to their high surface area. Many research types have shown that nanoparticles presence in the liquid enhances the fluid's thermal conductivity. It proves to be a better coolant for the automotive cooling system. In this research, a car radiator model was designed to simulate nonfluid flow in the radiator as a coolant. The simulation was first performed considering pure water as a coolant in the radiator and heat transfer was observed by viewing the coolant temperature throughout the flow regime. The heat transfer enhancement, a nanofluid was selected which is the suspension of nanoparticles in a particular base fluid. This research base fluids were ethylene glycol and water whereas the chosen nanoparticles are alumina ($AL_2O_3$). Simulation for mutually pure base fluid (water) and nanoparticle based fluid was performed and results were compared. It was found that the fluid having suspended nanoparticles showed higher conductivity which means that they have better heat transfer properties. The simulation results were also equated with the numerical consequences to check the validity of the proposed model. The effect of different concentrations of nano articles in the base fluid was also observed and eventually found that by the cumulative concentration of nanoparticles, better heat transfer may be achieved. This research also gives the idea of the compact design of the radiator. When nanofluids are used to intensifier the coolant heat transfer rate, means a constant heat transfer may be succeeded in a short length of the tube. In this way, the short length tubes may be used to cool down the coolant circulating within them.

## Acknowledgment

The authors would like to acknowledge the Department of Chemical Engineering and Department of Polymer and Petrochemical Engineering, NED University of Engineering & Technology, Karachi, Pakistan, for supporting this research work.

**Conflict of Interest.** The authors declare that they have no conflict of interest.

## References

Abhilash, P., Raghupathi, U., Kumar, P. 2021. Design and testing of radiator with fixed channel and helical pipe using nanofluids. In: *Proceeding of Materials Today International Conference on Advanced Materials and Modern Manufacturing*, pp. 615-620, Netherland Elsevier Publishing Company, Amsterdam, The Netherlands. https://doi.org/10.1016/j.matpr.2020.09.002

Abu-Hamdeh, N.H., Bantan, R.A.R., Alimoradi, A. 2020. Heat transfer optimization through new form of pin type of finned tube heat exchangers using the exergy and energy analysis. *International Journal of Refrigeration*, **117:** 12-22. https://doi.org/10.1016/j.ijrefrig.2020.03.023

Ahmed, W., Chowdhury, Z.Z., Kazi, S.N., Johan, M.R., Akram, N., Oon, C.S. 2020. Effect of ZnO-water based nanofluids from sonochemical synthesis method on heat transfer in a circular flow passage. *International Communications in Heat and Mass Transfer*, **114:** 1-13. https://doi.org/10.1016/j.icheatmasstransfer.2020.104591

Akbar, A., Firdaus, R., Cahyono, N. 2018. The cooling effectiveness of the V-ixion motorcycle radiator using water coolant variation. *IOP Conference Series: Materials Science and Engineering*, **434:** 1-5. https://doi.org/10.1088/1757-899X/434/1/012179

Al-Araji, K.M., Hachim, D.M., A, A.M. 2021. Nano Fluids as a coolant for automotive engine radiators: review study. *Al-Furat Journal of Innovations in Mechanical and Sustainable Energy Engineering*, **1:** 64-78. https://journals.atu.edu.iq/index.php/fjimse/article/view/86

Alqahtani, A.S., Alenazy, W.M., Pandiaraj, S. 2020. Optimization on heat transfer coefficient of plate heat exchanger using MWCNT-$TiO_2$ nanofluid by response surface methodology. *Materials Research Express*, **7:** 1-13. https://doi.org/10.1088/2053-1591/abaf8c

Awais, M., Saad, M., Ayaz, H., Ehsan, M.M., Bhuiyan, A.A. 2020. Computational assessment of nano particulate ($Al_2O_3$/water) utilization for enhancement of heat transfer with varying straight section lengths in a serpentine tube heat exchanger. *Thermal Science and Engineering Progress*, **20:** 1-15. https://doi.org/10.1016/j.tsep.2020.100521

Erdoðan, B., Zengin, Ý., Mert, S., Topuz, A., Engin, T. 2020. The experimental study of the entropy generation and energy performance of nanofluid flow for automotive radiators. *Engineering Science and Technology, An International Journal*, **24:** 1-10. https://doi.org/10.1016/j.jestch.2020.10.007

Goudarzi, K., Jamali, H. 2017. Heat transfer enhancement of $Al_2O_3$-EG nanofluid in a car radiator with wire coil inserts. *Applied Thermal Engineering*, **118:** 510-517. https://doi.org/10.1016/j.applthermaleng.2017.03.016

Goudarzi, K., Jamali, H., Kalaei, V. 2020. Heat transfer enhancement of car radiator using $Al_2O_3$/water nanofluid in the presence of electric field, an experimental study. *Advanced Energy Conversion Materials*, **1:** 15-24. https://doi.org/10.37256/aecm.112020110

Ijaz, H., Raza, H., Gohar, G.A., Ullah, S., Akhtar, A., Imran, M. 2020. Effect of graphene oxide doped nano coolant on temperature drop across the tube length and effectiveness of car radiator – A CFD study. *Thermal Science and Engineering Progress*, **20:** 1-8. https://doi.org/10.1016/j.applthermaleng.2017.03.016

Jaliliantabar, F., Ettefaghi, E., Mohtasebi, S.S., Jarrah, H.T. 2021. Experimental investigation of silver/water nanofluid heat transfer in car radiator. *Journal of Mechanical Engineering and Sciences*, **15:** 7743-7753. https://doi.org/10.15282/jmes.15.1.2021.10.0610

Karimi, A., Afrand, M. 2018. Numerical study on thermal performance of an air-cooled heat exchanger: effects of hybrid nanofluid, pipe arrangement and cross section. *Energy Conversion and Management*, **164:** 615-628. https://doi.org/10.1016/j.enconman.2018.03.038

Kocheril, R., Elias, J. 2020. Comparison of heat transfer rate with aluminium based nano fluid and magnetised ferro fluid in internal combustion engine heat exchanger. *Journal of Advanced Research in Fluid Mechanics and Thermal Sciences*, **67:** 170-177. http://akademiabaru.com/submit/index.php/arfmts/article/view/2844

Kumar, P.P., Krishna, P.V.S.M. 2017. Improving performance of automobile radiator by adding $Al_2O_3$(alumina)nanofluid to ethylene glycol based fluid coolant. *International Journal of Engineering Sciences and Research Technology*, **6:** 445-452. https://doi.org/10.5281/zenodo.573548

Li, X., Wang, H., Luo, B. 2021. The thermo physical properties and enhanced heat transfer performance of SiC-MWCNTs hybrid nanofluids for car radiator system. *Colloids and Surfaces A: Physicochemical and Engineering Aspects*, **612:** 1-10. https://doi.org/10.1016/j.colsurfa.2020.125968

Mandole, B.D., Mistry, T.S., Tayade, A.M., Ingale, A.P., Shinde, S. 2020. Review of nano fluids and its effect on heat transfer through radiator. *Mukt Shabd Journal*, **9:** 1811-1818. https://sersc.org/journals/index.php/IJFGCN/article/download/28428/15762

Mert, S., Yasar, H., Durmaz, U., Topuz, A., Yeter, A., Engin, T. 2021. An experimental study on cooling performance of a car radiator using $Al_2O_3$-ethylene glycol/water nanofluid. *Thermal Science*, **25:** 801-809. https://doi.org/10.2298/TSCI190630179M

Mohan, S.V., Kuriakose, J.R.A.N., Varghese, B.F.F. 2017. Experimental comparison of heat transfer in a down flow louvered fin Auto radiator using water, water and ethylene glycol mixture and water, ethylene glycol and sugarcane juice mixture as coolants. *Global Research and Development Journal for Engineering*, **2:** 215-223. https://doi.org/10.1016/j.icheatmasstransfer.2020.104591

Nagib, M., Elshamy, S.M., Zafan, H., Dadoura, H.H. 2019. Experimental study for enhancement the cooling system and exhaust gasses for gasoline automotive engine using nano-fluid. *Engineering Research Journal*, **161:** 1-15. https://doi.org/10.21608/ERJ.2019.139773

Patel, H.V., Subhedar, D.G., Ramani, D.B. 2017. Numerical investigation of performance for car radiator oval tube. In: *Proceedings of Materials Today International Conference on Recent Trends in Engineering and Material Sciences (ICEMS-2016)*, pp. 9384-9389, Jaipur, India. Elsevier Publishing Company, Amsterdam, The Neterlands. https://www.academia.edu/download/55487898/Pratik_Review.pdf.

Reddy, P.P.K., Reddy, A.B., Sudhakar, C. 2019. An experimental investigation on heat transfer in automobile radiator using the reinforcement of titanium dioxide nano fluid in coolant. *International Journal of Research in Advent Technology*, **10:** 52-57. https://www.academia.edu/download/60598119/COnf_Praveen20190914-111643-oe7el1.pdf.

Subhedar, D.G., Ramani, B.M., Gupta, A. 2018. Experimental investigation of heat transfer potential of $Al_2O_3$/water mono ethylene glycol nanofluids as a car radiator coolant. *Case Studies in Thermal Engineering*, **11:** 26-34. https://doi.org/10.1016/j.csite.2017.11.009

Patil, T.P., Pande, M., Chopade, D. 2017. Heat transfer enhancement in radiator by nanofluids - a review. *International Journal of Recent Engineering Research and Development*, **2:** 81-84. https://www.academia.edu/download/55487898/Pratik_Review.pdf

Vijayan, V.S.S., Antony, A.G., Loganathan, M., Baskar, S. 2019. Heat transfer enhancement in mini compact heat exchanger by using alumina nanofluid. *International Journal of Mechanical Engineering and Technology*, **10:** 564-570. http://www.iaeme.com/ijmet/issues.asp?JType=IJMET&VType=10&IType=1